Braiding and All Quantum Operations with Majorana Modes in 1D

Kornich, Viktoriia; Huang, Xiaoli; Repin, Evgeny; Nazarov, Yuli V.

DOI
10.1103/PhysRevLett.126.117701

Publication date
2021

Document Version
Final published version

Published in
Physical Review Letters

Braiding and All Quantum Operations with Majorana Modes in 1D

Viktoriia Kornich, Xiaoli Huang, Evgeny Repin, and Yuli V. Nazarov
Kavli Institute of Nanoscience, Delft University of Technology, 2628 CJ Delft, Netherlands

(Received 14 September 2020; accepted 12 February 2021; published 19 March 2021)

We propose a scheme to perform braiding and all other unitary operations with Majorana modes in one dimension that, in contrast to previous proposals, is solely based on resonant manipulation involving the first excited state extended over the modes. The detection of the population of the excited state also enables initialization and read-out. We provide an elaborated illustration of the scheme with a concrete device.

DOI: 10.1103/PhysRevLett.126.117701

The paradigm of topological quantum computation [1,2] provides an elegant solution to the most important problem in quantum manipulations: the decoherence problem. It implements a topologically protected degenerate ground state as a computational basis. The degenerate state can be visualized as a set of localized anyons while unitary operations are performed by adiabatic exchange of the anyons, that is, braiding of their world lines [2]. The braiding is feasible in two dimensions and impossible in one dimension since anyons should not collide in the course of operation. The intrinsically slow speed of adiabatic manipulation, as well as the difficulties of read-out and initialization of the protected states, should be compensated by the intrinsic fault tolerance of the operations.

Of all the numerous physical realizations of the topologically protected degenerate ground state proposed, the Majorana zero-energy states in hybrid semiconductor-superconductor devices [3,4] seems to be the most technologically advanced and elaborated. After pioneering experiments [5], an enormous outgoing research effort [6–8] resulted in considerable improvement of the technology and new observations, yet the quantum coherence in degenerate subspace still awaits experimental demonstration [9]. An obvious difficulty is that Majorana modes are realized in 1D nanowires, making direct braiding impossible. In principle, the 1D wires can be combined into a 2D network. There are elaborated schemes to realize braiding in various systems, for instance, in T or Y junctions of nanowires [10–16]. A enormous technological challenge to make such networks with necessary controls is being addressed [17], but the progress is slow so far.

In this Letter, we propose a scheme to realize Majorana braiding in a single 1D nanowire. Eventually, with this scheme one can realize any unitary transformation in the degenerate subspace, as well as initialization and readout in this subspace. The scheme uses resonant manipulation technique, the resonance being between the degenerate subspace and the lowest excited state that extends over all Majorana modes. The initialization and readout is possible if the population of the excited state is detected.

Strictly speaking, the scheme compromises the quantum computation paradigm since the topological protection fails during the operation. The system is subject to relaxation while being in the excited state. There are standard means to reduce this only source of decoherence, for instance, photonic [18–20] and phononic [21–24] cavities and metamaterials, and make the operation time shorter than the corresponding relaxation time. It is important that the protection is preserved between the operations. This makes the scheme an ideal tool to demonstrate persistence of quantum superpositions in the degenerate subspace, and quantify the macroscopically long decoherence time expected. In the final part of the Letter, we discuss the use of the scheme in wider context. We illustrate the scheme on the example of a minimum concrete setup, at a general level as well as with a concrete microscopic model and numbers.

The setup under consideration (Fig. 1) encompasses a finite 1D wire brought in proximity with a superconductor.

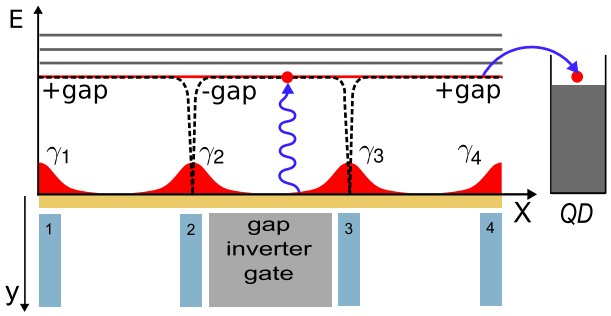

FIG. 1. The setup for the resonant manipulation of Majorana modes. The proximitized nanowire (orange rectangle) with the inverted gap in the middle section hosts four Majorana modes (γ_{1-4}) formed on the edges of the sections of different topology. The four gates in the vicinity of the modes are used to apply a pulse sequence for the resonant manipulation, the resonance being with the lowest excited state (red line) extented over the modes. A quantum dot on the left can be used to detect the population of the excited state.

It hosts 4 localized Majorana modes, two at the ends and two in the middle. This is achieved by a gap inversion in the middle section of the wire by a nearby gate. The wire sections at the sides are thus in a topological regime of parameters while the middle section is topologically trivial. It is important for us that the first excited state right above the gap extends over the whole wire. This is achieved by matching the absolute values of the gap in the middle and side sections by the gap inverter gate. To achieve efficient resonant manipulation, we require four more gates near the positions of Majorana modes. This is all we need for resonant manipulation. To detect a possible quasiparticle in the excited state, we put a quantum dot nearby (it can be in the same nanowire, as presented in Refs. [25,26]). The addition energy of the dot is tuned such that a quasiparticle in the excited state tunnels to the dot changing its charge, which is measured. For effective detection, the tunnel rate should exceed the relaxation rate. The tunnel coupling can be switched on only for duration of measurement.

To start with, let us understand the basis involving the Majorana modes and the first excited state. Let $c_L = (\gamma_1 + i\gamma_2)/2$, $c_R = (\gamma_3 + i\gamma_4)/2$ be the quasiparticle annihilation operators in Majorana subspace, and $c_{\rm ex}$ to be that in the excited state. A basis state is defined as $|n_L, n_R\rangle|n_{\rm ex}\rangle$, where $n_L, n_R, n_{\rm ex} = 0, 1$ are the respective occupation numbers. We thus have 8 states. They separate into two groups of four corresponding to two possible total parities. There can be no coherence between the states of different parities. We define the bases as follows:

$$\Phi_e = \{|00\rangle|0\rangle, |11\rangle|0\rangle, |01\rangle|1\rangle, |10\rangle|1\rangle\}, \tag{1}$$

for the even parity, and

$$\Phi_o = \{|01\rangle|0\rangle, |10\rangle|0\rangle, |00\rangle|1\rangle, |11\rangle|1\rangle\}, \tag{2}$$

for the odd parity. The first two states for each parity form Majorana subspace. We can thus realize a Majorana qubit for each parity. We would like to perform unitary operations in Majorana subspace. A particular unitary operation is a braiding of two Majorana modes defined as $U_{ij} = \frac{1}{\sqrt{2}}(1 + \gamma_i\gamma_j)$. For instance, the braiding of the second and the third mode in the odd basis Φ_e is given by

$$U^o_{23} = \frac{1}{\sqrt{2}}(1 + \gamma_2\gamma_3) = \frac{1}{\sqrt{2}}\begin{pmatrix} 1 & i & 0 & 0 \\ i & 1 & 0 & 0 \\ 0 & 0 & 1 & i \\ 0 & 0 & i & 1 \end{pmatrix}. \tag{3}$$

As we see, it is separated into blocks of Majorana and excited subspace, as these operations are independent. Since we wish to operate in Majorana subspace, the excited block is irrelevant. The corresponding matrix in the even subspace is obtained from Eq. (3) by the following transformation

$$U^e = \Sigma_y\sigma_y U^{o*}\sigma_y\Sigma_y, \tag{4}$$

σ_y, Σ_y being Pauli matricies acting within and over the blocks, respectively. Eventually, this relation holds for all braidings as well as for any 4×4 matrix we consider here. So we wish to perform braidings, as well as any unitary operations in Majorana subspace. This task by its own is senseless unless we have means to initialize to a state in this subspace and measure the result. Let us see how we can realize this by resonant manipulation.

A resonant manipulation is performed by applying the oscillating voltages to the gates 1–4 with the frequency matching the energy spacing. At constant amplitudes, the general Hamiltonian in rotating wave approximation reads

$$H_{\rm rm} = (\alpha_1 c_L + \alpha_2 c_R + \alpha_3 c_L^\dagger + \alpha_4 c_R^\dagger)c_{\rm ex} + \text{H.c.} \tag{5}$$

The four complex coefficients α_{1-4}, are in linear relation with the four complex voltage amplitudes at the gates, so 4 gates suffice to control all coefficients. Applying a pulse of duration t makes a unitary operation $U = e^{-iH_{\rm rm}t}$ in an eight-dimensional basis. The manipulation conserves parity, so the matrix separates in two 4×4 blocks U_e, U_o in the bases Φ_e, Φ_o. It is simple and important to show that these matrices satisfy the same relation (4) as the braiding matrices.

Let us stress that our aim is to find a unitary transformation that works in Majorana subspace only. To this end, we require a special form of the resulting U: that separated in two 2×2 blocks, like in Eq. (3). In other words, the excited state should not be populated at the end of the resonant manipulation if we start in Majorana subspace. This is impossible to achieve with a single pulse. A key observation is that this can be achieved combining *several* pulses. Two pulses with 8 complex parameters in total in principle suffice to realize our aim: an arbitrary 2×2 unitary transformation in Majorana basis. We describe the concrete methods of the pulse design and give examples further in the text.

Let us describe the protocol for initialization and readout starting from an unknown state of unknown parity in Majorana subspace. We will show that this requires two resonant pulse sequences, that is, unitary transformations, and a measurement after each sequence. We dub these sequences a developer and a fixer. To start with, let us assume that we start in a Majorana state of even parity. Let us understand the effect of the following 4×4 unitary transformation:

$$\begin{aligned} D^e = {} & |B\rangle|1\rangle\langle a|\langle 0| + |b\rangle|0\rangle\langle a'|\langle 0| \\ & + |B'\rangle|1\rangle\langle A|\langle 1| - |b'\rangle|0\rangle\langle A'|\langle 1|. \end{aligned} \tag{6}$$

Here, lowercase letters denote the Majorana states in the even subspace ($|00\rangle$, $|11\rangle$ or their linear combination) while capital ones denote those in the odd subspace ($|01\rangle$, $|10\rangle$ or their linear combination). The prime denotes a

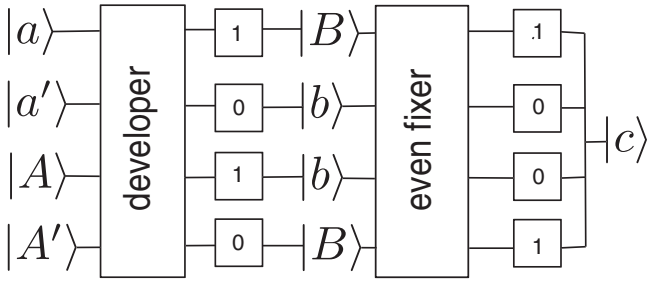

FIG. 2. Initialization and readout in Majorana subspace is achieved by two resonant pulse sequences: developer and fixer, and subsequent measurements of the excited quasiparticle. Uppercase and lowercase letters refer to Majorana superpositions of odd and even parity, respectively, prime indicates orthogonality, $\langle a'|a\rangle = 0$. The measurement outcomes are in square boxes. The protocol brings the system to the state $|c\rangle$ from an unknown state. The probabilities of the measurement outcomes give the probabilities of the states $|a\rangle, |a'\rangle, |A\rangle, |A'\rangle$. See the text for details.

corresponding orthogonal state, $|a'\rangle \equiv (i\sigma_y|a\rangle)^*$, $\langle a|a'\rangle = 0$ (note that $i\sigma_y i\sigma_y|a\rangle = -|a\rangle$). If the initial state is $|a\rangle$, this developer brings the system to the excited subspace. The quasiparticle tunnels to the dot, we measure outcome "1" and the system is in the state of the opposite parity, $|B\rangle|0\rangle$ (Fig. 2). If the initial state is orthogonal, no excitation occurs, we measure output "0" and get to the state $|b\rangle|0\rangle$. We see that the developer can be used to measure the probability of $|a\rangle$ if the initial parity is known to be even, and the final state is known from the measurement result. However, the parity is generally unknown.

Let us see how the same developer works in the odd subspace. We apply Eq. (4) to obtain

$$D^o = -|B'\rangle|0\rangle\langle a'|\langle 1| - |b'\rangle|1\rangle\langle a|\langle 1| - |B\rangle|0\rangle\langle A'|\langle 0| + |b\rangle|1\rangle\langle A|\langle 0|. \quad (7)$$

We see that now the developer tries to distinguish between $|A\rangle$ and $|A'\rangle$, while the final states for the same output are opposite: $|b\rangle|0\rangle$ for 1 and $|B\rangle|0\rangle$ for 0. Thus, we do not know the final state if the parity is unknown, neither we know which state has been measured.

However, the situation can be fixed if we apply another unitary transformation. While this transformation does *not* depend on the result of the first measurement, it depends on the desired parity of the final state. In any case, the incoming states of a fixer are the same as the output states of the developer in the Majorana subspace. Let us consider the even fixer F_e first. Its representation for two parities reads

$$F_e^e = |c\rangle|0\rangle\langle b|\langle 0| + |C\rangle|1\rangle\langle b'|\langle 0| + |C'\rangle|1\rangle\langle B|\langle 1| + |c'\rangle|0\rangle\langle B'|\langle 1|, \quad (8)$$

$$F_e^o = |c'\rangle|1\rangle\langle b'|\langle 1| + |C'\rangle|0\rangle\langle b|\langle 1| - |C\rangle|0\rangle\langle B'|\langle 0| - |c\rangle|1\rangle\langle B|\langle 0|. \quad (9)$$

After the fixer, and the second measurement, the final state is always $|c\rangle|0\rangle$, this solves the initialization task. If the outcomes of the first and second measurements are "11" or "00," the initial parity was even. Otherwise, it was odd.

The odd fixer F_o has a similar structure,

$$F_o^e = |C\rangle|1\rangle\langle b|\langle 0| + |c\rangle|0\rangle\langle b'|\langle 0| + |c'\rangle|0\rangle\langle B|\langle 1| + |C'\rangle|1\rangle\langle B'|\langle 1|, \quad (10)$$

$$F_o^o = -|C'\rangle|0\rangle\langle b'|\langle 1| - |c'\rangle|1\rangle\langle b|\langle 1| + |c\rangle|1\rangle\langle B'|\langle 0| + |C\rangle|0\rangle\langle B|\langle 0|. \quad (11)$$

In any case, the final state is $|C\rangle|0\rangle$. The measurement outcomes 11 and 00 manifest even initial parity, 01 and 10 manifest odd initial parity. So both fixers not only solve the initialization task: they determine the initial parity.

We see that the protocol described at the same time provides a measurement tool. Suppose we are able to arrange an unknown state of unknown parity, and reproduce it on demand. To characterize the state, one just repeats the protocol collecting the statistics of outcomes. The probabilities of outcomes 11,00,10,01 give the probabilities of the basis states $|a\rangle, |a'\rangle, |A\rangle, |A'\rangle$, respectively. The developer and fixer pulse sequences can be designed and realized for any choice of the superpositions $|a\rangle, |b\rangle, |c\rangle, |A\rangle, |B\rangle, |C\rangle$. In the Supplemental Material [27], we provide the concrete choice example.

To show the feasibility of the setup and the suggested pulse sequence design, we now specify a microscopic model and provide extensive numerical study for a concrete set of parameters. We make use of the Hamiltonian [3,4] to model a semiconducting nanowire with spin-orbit spectrum splitting, in the presence of applied uniform magnetic field B, and proximity-induced superconducting gap Δ. The gap inverter gate is described by a coordinate-dependent potential $\mu(x)$ such that its values in the middle and outer sections, μ_m, μ_o satisfy the conditions of trivial $B < \sqrt{\Delta^2 + \mu_m^2}$ and nontrivial $B > \sqrt{\Delta^2 + \mu_o^2}$ topology. The modulation gates are described by a time-dependent addition $\mu(x,t) = \sum_i V_i(t)\Theta(x - x_i)\Theta(y_i - x)$, x_i, y_i giving the start and end position of the gate i (see Fig. 3). The Hamiltonian in use reads

$$H_0 = \int dx \Psi^\dagger(x)\left[\left(-\frac{1}{2m}\frac{\partial^2}{\partial x^2} - i\alpha_{SOI}\sigma_z\frac{\partial}{\partial x} - \mu(x)\right)\tau_z + B\sigma_x + \Delta\tau_x\right]\Psi(x),$$
$$\Psi(x) = \{\psi_\uparrow(x), \psi_\downarrow(x), \psi_\downarrow^\dagger(x), -\psi_\uparrow^\dagger(x)\}, \quad (12)$$

$\psi_\sigma(x)$ being the electron field operators.

We measure length and energy in units of $(m\alpha_{\mathrm{SOI}})^{-1}$ and $m\alpha_{\mathrm{SOI}}^2$, respectively. We compute the spectrum and wave functions diagonalizing the discrete-in-space

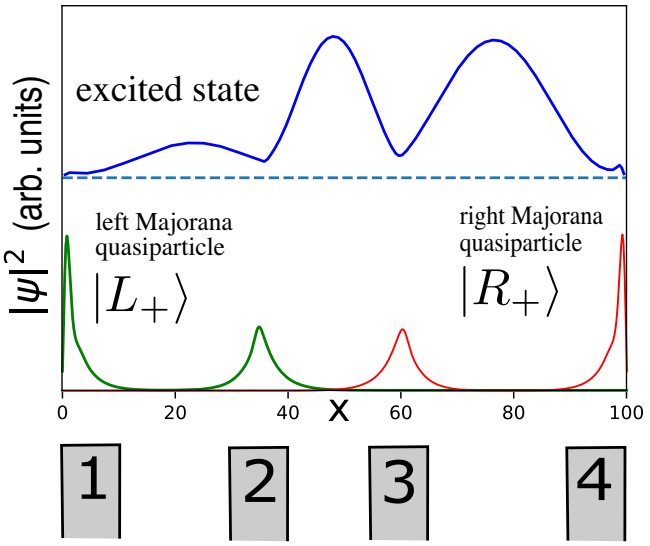

FIG. 3. The concrete illustrative setup. The probability densities of eigenfunctions and the positions of modulation gates 1–4 chosen at [0; 10], [30; 40], [55; 65], and [90; 100].

approximation of the Hamiltonian (12), with the discretization step 0.2. We choose a relatively long wire with length $L = 100$ and the material parameters are of the order of 1: $B = 3$, $|\Delta| = 2.5$, $\mu_m = -1.91$, $\mu_o = -1.34$, see Ref. [27] for details. The transition between these two values are smoothed at the length scale of 3, and the setup has been made slightly asymmetric. The bulk energy gaps corresponding to these parameters are $G_e = 0.146$ and $G_m = 0.164$, they are not precisely equal because of the finite size of the middle section. With this, the lowest excited state at $E_1 = 0.175$ is extended over the wire (see Fig. 3). Higher excited states are situated at $E_2 = 0.180$ and $E_3 = 0.187$. For the resonant signal to address the lowest excited state only, the inverse pulse duration should not exceed the level spacing $E_2 - E_1$, this gives $t > 10^3$.

The wave functions are presented in Fig. 3. There are 4 Majorana localized modes with the width ≈5. We neglect a marginal overlap between the states setting them at zero energy. The wave function of the first excited state reminds the first particle-in-the box state with noticeable dips owing to orthogonality with Majorana peaks, and is extended over the whole length of the wire. With these wave functions, we compute the matrix elements of voltages applied to 4 gates whose positions are given in Fig. 3. This gives as a 4×4 matrix $\hat{M}$ that relates the voltage amplitudes and the resonant manipulation coefficients α_i [Eq. (5)]. To design a pulse sequence corresponding to a unitary operation, we compute the resulting matrix depending on the parameters α_i and time duration of each pulse, and iteratively minimize in α_i the distance between the resulting and target matrix. Using the matrix $\hat{M}$, we convert to the gate voltage amplitudes. The design for the braiding of the second and the third Majorana mode is presented in Fig. 4, extensive examples are to be found in Ref. [27].

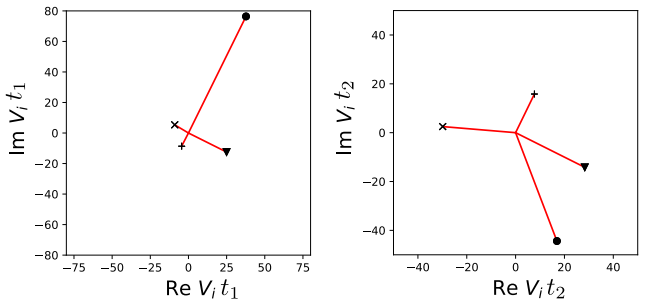

FIG. 4. Designed two-pulse sequence for the braiding U_{23}. The gate voltage amplitudes V_{1-4} times pulse durations $t_{1,2}$ are given by circle, plus sign, triangle, and x mark, respectively.

To conclude, we propose a scheme that allows us to realize braiding and all other unitary operations, as well as the measurement and initialization, for a Majorana qubit in a single 1D wire. It suits ideally to demonstrate macroscopically long coherence in Majorana space. The topological protection fails only during the operation. We illustrate the scheme with a concrete elaborated example.

Let us shortly present necessary discussions in a wider context. No experimental system can be modeled with the accuracy we did. However, to design the pulse sequencies, one only needs E_1 and the matrix M: the latter can be determined from the analysis of the spectra of the dressed resonant state at varying V_i. The resonance with the lowest state only is essential since it minimizes dissipation. Moreover, the excitation to many excited states is exponentially suppressed owing to destructive interference. The scheme can be readily extended to *more* Majorana modes within the single wire, like proposed in Refs. [9,28]. While this can be done with a single state extended over the wire, but a simpler design would involve separate excited states, each extended over a group of Majorana modes. This can be achieved by proper profile of $\mu(x)$. At the moment, the technological efforts are aimed to increase transparency of the barrier between the wire and the superconductor. As it is shown, for instance, in Ref. [29] at sufficiently high transparency the wire is not described by the Hamiltonian [3,4] and eventually looses the localized excited states. So the moderate transparency is required for experimental realization of our idea. The idea presented may be also useful in the context of more traditional 2D Majorana braiding: one can set a localized excited state, switch on a resonant field, and move the modes passing the state to achieve the resonant manipulation and read out.

The data that support the findings of this study are available in Ref. [30].

We acknowledge useful discussions with Anton Akhmerov, Kim Pöyhönen, and Felix von Oppen. This project has received funding from the European Research

Council (ERC) under the European Union's Horizon 2020 research and innovation programme (Grant Agreement No. 694272) and was supported by the Netherlands Organisation for Scientific Research (NWO/OCW), as part of the Frontiers of Nanoscience (NanoFront) program.

[1] A. Kitaev, Ann. Phys. (Amsterdam) **303**, 2 (2003).
[2] C. Nayak, S. H. Simon, A. Stern, M. Freedman, and S. Das Sarma, Rev. Mod. Phys. **80**, 1083 (2008).
[3] R. M. Lutchyn, J. D. Sau, and S. Das Sarma, Phys. Rev. Lett. **105**, 077001 (2010).
[4] Y. Oreg, G. Refael, and F. von Oppen, Phys. Rev. Lett. **105**, 177002 (2010).
[5] V. Mourik, K. Zuo, S. M. Frolov, S. R. Plissard, E. P. A. M. Bakkers, and L. P. Kouwenhoven, Science **336**, 1003 (2012).
[6] M. T. Deng, C. L. Yu, G. Y. Huang, M. Larsson, P. Caroff, and H. Q. Xu, Nano Lett. **12**, 6414 (2012).
[7] A. Das, Y. Ronen, Y. Most, Y. Oreg, M. Heiblum, and H. Shtrikman, Nat. Phys. **8**, 887 (2012).
[8] A. D. K. Finck, D. J. Van Harlingen, P. K. Mohseni, K. Jung, and X. Li, Phys. Rev. Lett. **110**, 126406 (2013).
[9] H. Zhang, D. E. Liu, M. Wimmer, and L. P. Kouwenhoven, Nat. Commun. **10**, 5128 (2019).
[10] J. Alicea, Y. Oreg, G. Refael, F. von Oppen, and M. P. A. Fisher, Nat. Phys. **7**, 412 (2011).
[11] F. Harper, A. Pushp, and R. Roy, Phys. Rev. Research **1**, 033207 (2019).
[12] Z.-C. Yang, T. Iadecola, C. Chamon, and C. Mudry, Phys. Rev. B **99**, 155138 (2019).
[13] T. Posske, C.-K. Chiu, and M. Thorwart, Phys. Rev. Research **2**, 023205 (2020).
[14] D. Aasen, M. Hell, R. V. Mishmash, A. Higginbotham, J. Danon, M. Leijnse, T. S. Jespersen, J. A. Folk, C. M. Marcus, K. Flensberg, and J. Alicea, Phys. Rev. X **6**, 031016 (2016).
[15] D. J. Clarke, J. D. Sau, and S. Das Sarma, Phys. Rev. B **95**, 155451 (2017).
[16] C. W. J. Beenakker, SciPost Phys. Lect. Notes **15** (2020), https://scipost.org/SciPostPhysLectNotes.15.
[17] S. Gazibeg1ovic *et al.*, Nature (London) **548**, 434 (2017).
[18] E. Yablonovitch, Phys. Rev. Lett. **58**, 2059 (1987).
[19] N. I. Zheludev and Y. S. Kivshar, Nat. Mater. **11**, 917 (2012).
[20] A. Blais, R.-S. Huang, A. Wallraff, S. M. Girvin, and R. J. Schoelkopf, Phys. Rev. A **69**, 062320 (2004).
[21] Y. Pennec, J. O. Vasseur, B. Djafari-Rouhani, L. Dobrzyński, and P. A. Deymier, Surf. Sci. Rep. **65**, 229 (2010).
[22] P. A. Deymier, *Acoustic Metamaterials and Phononic Crystals* (Springer Science, Berlin, 2013), Vol. 173.
[23] A. Khelif and A. Adibi, *Phononic Crystals: Fundamentals and Applications* (Springer, New York, 2016).
[24] V. Laude, *Phononic Crystals: Artificial Crystals for Sonic, Acoustic, and Elastic Waves* (De Gruyter, Berlin, 2015).
[25] M.-T. Deng, S. Vaitiekėnas, E. Prada, P. San-Jose, J. Nygård, P. Krogstrup, R. Aguado, and C. M. Marcus, Phys. Rev. B **98**, 085125 (2018).
[26] E. Prada, R. Aguado, and P. San-Jose, Phys. Rev. B **96**, 085418 (2017).
[27] See Supplemental Material at http://link.aps.org/supplemental/10.1103/PhysRevLett.126.117701 for additional details and calculations regarding the example setup under consideration, as well as concrete designs of unitary transformations for quantum manipulation, initialization, and measurement.
[28] S. Das Sarma, J. D. Sau, and T. D. Stanescu, Phys. Rev. B **86**, 220506 (2012).
[29] T. D. Stanescu, R. M. Lutchyn, and S. Das Sarma, Phys. Rev. B **84**, 144522 (2011).
[30] E. Repin, V. Kornich, X. Huang, and Y. V. Nazarov, https://doi.org/10.5281/zenodo.4377165 (2020).